RHEUMATOLOGY

Rheumatology 2010;49:1852–1861
doi:10.1093/rheumatology/keq188
Advance Access publication 26 June 2010

Original article

Angiogenesis and nerve growth factor at the osteochondral junction in rheumatoid arthritis and osteoarthritis

David A. Walsh[1,2], Dan F. McWilliams[1], Matthew J. Turley[1], Madeleine R. Dixon[1], Rebecca E. Fransès[1], Paul I. Mapp[1] and Deborah Wilson[2]

Abstract

Objectives. The osteochondral junction can be a source of pain in both RA and OA. Growth of blood vessels and nerves from the subchondral bone into articular cartilage may mediate the association between joint pathology and symptoms. We have investigated associations between angiogenesis, inflammation and neurovascular growth factor expression at the osteochondral junction in human arthritis.

Methods. Osteochondral junctions from medial tibial plateaux of patients undergoing arthroplasty for RA ($n = 10$) or OA ($n = 11$), or from non-arthritic post-mortem controls ($n = 11$) were characterized by immunohistochemistry for CD34 and smooth muscle α-actin (blood vessels), CD68 (macrophages), CD3 (lymphocytes), proliferating cell nuclear antigen, vascular endothelial, platelet-derived and nerve growth factor (NGF).

Results. Osteochondral angiogenesis was demonstrated as increased endothelial cell proliferation and vascular density in non-calcified articular cartilage, both in RA and OA. Osteochondral angiogenesis was associated with subchondral bone marrow replacement by fibrovascular tissue expressing VEGF, and with increased NGF expression within vascular channels. RA was characterized by greater lymphocyte infiltration and PDGF expression than OA, whereas chondrocyte expression of VEGF was a particular feature of OA. NGF was observed in vascular channels that contained calcitonin gene-related peptide-immunoreactive sensory nerve fibres.

Conclusions. Osteochondral angiogenesis in RA and OA is associated with growth factor expression by cells within subchondral spaces, vascular channels and by chondrocytes. NGF expression and sensory nerve growth may link osteochondral angiogenesis to pain in arthritis.

Key words: Rheumatoid arthritis, Osteoarthritis, Subchondral bone, Inflammation, Pathological neovascularization, Nerve growth, Calcitonin gene-related peptide, Knee, Immunohistochemistry.

BASIC SCIENCE

Introduction

Subchondral pathology may importantly contribute to both RA and OA. Subchondral inflammatory infiltrates in RA contain lymphocytes, produce chemokines and MMPs [1, 2], and are osteoclastic [2–4]. In OA, subchondral bone plate thickening may stress and damage the overlying cartilage [5], and may impair nutrition to its deeper layers [6]. OA and RA both result in chondropathy, and RA leads eventually to secondary OA, identifiable by the development of marginal osteophytes (OSTs) [7]. In both OA and RA, subchondral bone may be a source of pain [8–10].

Loss of integrity of the osteochondral junction is described in both RA and OA, attributed in RA to 'subchondral erosions' [1, 11, 12] and in OA described as 'vascular channels', both indicating subchondral bone remodelling [5, 8, 13–15]. Blood vessels are localized to channels that breach the osteochondral junction, but are rarely found

[1]Arthritis Research UK Pain Centre, Division of Academic Rheumatology, University of Nottingham, Nottingham City Hospital, Nottingham and [2]Department of Rheumatology, Sherwood Forest Hospitals NHS Trust, Sutton in Ashfield, UK.

Submitted 12 November 2009; revised version accepted 14 May 2010.

Correspondence to: David A. Walsh, Arthritis Research UK Pain Centre, Division of Academic Rheumatology, University of Nottingham, Clinical Sciences Building, Nottingham City Hospital, Hucknall Road, Nottingham NG5 1PB, UK. E-mail: david.walsh@nottingham.ac.uk

in normal articular cartilage beyond the tidemark [8, 16, 17]. Fine, unmyelinated sensory nerves accompany blood vessels within vascular channels and may contribute to pain in OA [8, 10]. The factors that lead to the vascularization and innervation of the articular cartilage in human arthritis are little understood.

Synovitis is not only characteristic of RA, but also a key feature of OA [18]. Subchondral inflammation is well described in RA [1, 2], and may also be a feature of OA, where fibrovascular tissue replaces fatty bone marrow [19]. These expansile, proliferating lesions may extend to communicate with the articular surface, and may be associated with bone marrow lesions observed by MRI [20], and with subchondral cytokine and MMP expression [21].

Synovial angiogenesis is associated with, and apparently dependent on, inflammation, both in RA and OA [16, 18, 22]. However, osteochondral angiogenesis was associated with chondropathy rather than synovitis in OA [16, 23], indicating that osteochondral and synovial angiogenesis are concurrent but differentially regulated processes. Subchondral inflammation and neovascularization have been noted to co-exist in RA [1, 2], but a possible contribution of subchondral inflammation to osteochondral angiogenesis has received little attention.

VEGF and PDGF are important mediators of blood vessel growth. VEGF stimulates endothelial cell (EC) proliferation and migration, and stabilizes newly formed blood vessels, whereas PDGF recruits pericytes and smooth muscle cells, leading to vascular maturation [24]. Sensory nerve growth is stimulated by nerve growth factor (NGF), which is also up-regulated in inflamed synovium [25]. NGF can also stimulate angiogenesis, demonstrating the often close link between blood vessel and nerve growth [26]. It is unknown, however, whether these same factors are available to stimulate osteochondral, as well as synovial angiogenesis and nerve growth.

We hypothesized that osteochondral angiogenenesis and sensory nerve growth are driven by growth factors produced by cells within the subchondral bone spaces and vascular channels. By comparing tibiofemoral samples from patients with RA or OA with those from post-mortem (PM) controls, we characterized the subchondral cellular milieu and investigated possible associations with vascular growth.

Methods

Patient samples

Patients fulfilled the ARA criteria for RA ($n = 10$, two males) or OA ($n = 11$, eight males). PM controls ($n = 11$, five males) had macroscopically normal tibial plateaux and no visible OSTs. Additional samples from three patients (PM; $n = 2$, OA; $n = 1$, all males) were processed to permit evaluation of the relative distributions of NGF- and calcitonin gene-related peptide (CGRP) immunoreactivities. Written consent was obtained from all patients or, for PM cases, next of kin [27], according to the Declaration of Helsinki. The study was approved by the UK National Research Ethics Service or its predecessors (reference numbers NNHA/420, NNHA/544, NNHA/673 and 05/Q2403/24, 05/Q2403/61 and 08/H0403/13). Postero-anterior knee radiographs were allocated scores for joint space narrowing (JSN) and osteophytosis using a standardized line atlas [28].

Formalin-fixed coronal sections of the middle third of medial tibial plateaux were decalcified in 10% EDTA in 10 mM Tris buffer (pH 6.95, room temperature) and then were wax embedded. Decalcification was confirmed by radiography. Samples used for co-localization of CGRP-immunoreactive nerves with NGF were fixed by the method of Zamboni [29], using a solution of 2% (w/v) paraformaldehyde, 15% (v/v) picric acid in phosphate buffer (pH 7.3) overnight at 4°C, and then transferred to 15% (w/v) sucrose in phosphate buffered saline (PBS/sucrose) solution at 4°C for 5 days. Zamboni's fixed tissues were decalcified as above, except at 4°C, then immersed and frozen in optimal cutting temperature and stored at −80°C.

Histomorphometry

Sections were cut with a thickness of 5 μm, or, for CGRP- and NGF-co-localization, 20 μm. Immunoreactivities were detected without (VEGF, NGF, CGRP and α-actin) or after (CD3, CD68 and PDGF-B) antigen retrieval, respectively, in 10 mM Tris/1 mM EDTA (pH 9.0, 95°C for 20 min), or 1 mg/ml pepsin in 0.5 M acetic acid (37°C for 2 h) or 10 mM citrate buffer (pH 6, 95°C for 20 min). Proliferating ECs were visualized following antigen retrieval in 10 mM citrate buffer (pH 6, 90°C for 5 min), using double-sequential immunohistochemistry for proliferating cell nuclear antigen (PCNA; clone PC10) and CD34 [22]. Visualization used avidin–biotin complex (ABC)-peroxidase or -alkaline phosphatase and diaminobenzidine (DAB) alone or with nickel enhancement [30] or FastRed™.

All histomorphometry were performed blinded to diagnostic group, by methods appropriate to the distribution of staining, based on initial qualitative analyses. Samples without articular cartilage were excluded from analysis.

Vascular density/millimetre tidemark was determined as channels (20–120 μm wide) terminating in the subchondral bone, calcified cartilage and non-calcified cartilage. Subchondral bone plate thickness was subchondral bone plate sectional area [measured using a KS300 computer-assisted image analysis system (Imaging Associates, Bicester, UK)], divided by tidemark length (measured by digital caliper; Mitutoyo, Andover, UK). Subchondral bone plate area included spaces occupied by vascular channels and excluded subchondral bone spaces. OA severity (chondropathy) score was modified from Mankin, excluding tidemark integrity (possible range 0–13) [8, 14, 16].

CD3-immunoreactive cells were graded in subchondral bone as: 0, none; 1, $\geqslant 1$ cell not dispersed widely; and 2, positive cells widely dispersed. VEGF-immunoreactive cells were graded in subchondral bone as: 0, none; 1, $\leqslant 10\%$; and 2, $>10\%$ of cells; and in vascular channels as occupying: 0, $<20\%$; 1, 20–70%; and 2, $>70\%$ of

channels. PDGF immunoreactivity was graded in vascular channels as occupying: 0, none; 1, <50%; and 2, ⩾50% of channels. CD68-positive mononuclear cells were graded in the subchondral bone as: 0, none; 1, focal/sparse distribution; and 2, high density; and in vascular channels as occupying: 0, none; 1, <1%; 2, 1–5%; and 3, >5% of channel section area. NGF expression was measured as proportion of vascular channels displaying positive cells.

Statistical analysis

Data were analysed with Statistical Package for Social Sciences, version 14 (SPSS Inc., Chicago, IL, USA), using Kruskal–Wallis test with *post hoc* Mann–Whitney U-test, Spearman's rank correlation coefficients or χ^2 statistic. $P < 0.05$ after correction for multiple comparisons indicated statistical significance. Data are median and interquartile range (IQR).

Materials

Mouse mABs to CD34 (QBEnd10), CD3 (F7.2.38) and CD68 (PG-M1) were from DakoCytomation (Cambridge, UK), and to α-actin (1A4) from Sigma Chemical Co. (Poole, UK). Rabbit polyclonal anti-PDGF (H55), anti-VEGF (A20) and anti-NGF (H-20) were from Santa Cruz Biotechnology, Inc. (Santa Cruz, CA, USA). Rabbit polyclonal anti-CGRP (T-4239) was from Peninsula Laboratories (Belmont, CA, USA). Biotinylated secondary antibodies, Vectastain ABC-peroxidase Elite and ABC-alkaline phosphatase were from Vector Laboratories Ltd (Peterborough, UK). Mayer's haematoxylin and eosin were obtained from Raymond A. Lamb Ltd (East Sussex, UK). Ammonium chloride, DePeX mounting medium, Superfrost Plus microscope slides, PBS (pH 7.5) and $CaCl_2$ were from VWR International Ltd (Lutterworth, UK). Orthophosphate buffered formalin was from Cell Path PLC (Wales, UK). All other chemicals and reagents were from Sigma Chemical Co (Poole, UK).

Results

Patient details

Radiographic severity (Table 1) and disease duration were similar in RA and OA, with 8 (RA) and 10 (OA) patients reporting disease for >5 years. All RA cases displayed tibiofemoral OSTs on radiographs. Effusion was detected in the index knee of six patients with RA and five with OA. Disease-modifying anti-rheumatic agents were used by eight patients with RA (seven MTX, three ciclosporin and one SSZ), oral corticosteroids by five patients (four RA and one PM), bisphosphonates by two and oestrogens by a further one patient with RA.

General morphology

Morphology of the tibial plateaux (Table 1 and Fig. 1) was as previously reported [16]. Articular cartilage displayed varying degrees of chondropathy. The subchondral bone plate was of variable thickness and subchondral bone spaces were occupied by soft tissue of two predominant types: fatty tissue containing bone marrow or fibrovascular tissue containing matrix, mononuclear and vascular cells (Fig. 1A). Chondropathy, subchondral bone thickness and fibrovascular marrow replacement each displayed heterogeneity between disease groups ($\chi^2 = 8.2$, $P = 0.017$; $\chi^2 = 7.7$, $P = 0.021$; and $\chi^2 = 10.5$, $P = 0.005$, respectively). RA cases displayed greater chondropathy, thinner subchondral bone plates and more frequent fibrovascular marrow replacement than PM, with intermediate values in OA (Table 1).

Osteochondral vascularity

CD34-positive cells and smooth muscle α-actin-positive cells were each organized in luminated vessel-like structures, often containing erythrocytes, consistent with EC and pericyte/vascular smooth muscle cell morphology (Fig. 1B and C). Blood vessels were observed within both marrow and fibrovascular types of subchondral tissue and in vascular channels. Vascular channels were observed in all disease groups as extensions of the subchondral bone spaces. PCNA-positive ECs were observed in vessels within subchondral bone spaces and in vascular channels, often alongside PCNA-positive non-vascular cells (Fig. 1C).

Numbers of vascular channels terminating in the non-calcified articular cartilage or in the subchondral bone displayed heterogeneity between disease groups ($\chi^2 = 10.2$, $P = 0.006$ and $\chi^2 = 9.1$, $P = 0.01$, respectively). Vascular densities for OA and RA cases were higher in the non-calcified cartilage, and lower in the subchondral bone than for PM cases (Table 1). Presence of proliferating ECs within vascular channels that breached the tidemark displayed heterogeneity between disease groups ($\chi^2 = 6.7$, $P = 0.04$; Fig. 1C and Table 1). RA cases were more likely to display proliferating ECs in vascular channels than were PM cases ($Z = -2.0$, $P = 0.02$). Cases that displayed PCNA-positive ECs within vascular channels displayed higher vascular densities within the non-calcified cartilage [0.85 (0.57–1.1) per mm] than did those without evidence of EC proliferation [0.16 (0.11–0.34) per mm, $Z = 3.2$, $P = 0.001$].

High vascular density in the non-calcified cartilage was associated with greater chondropathy and fibrovascular marrow replacement (Table 2). EC proliferation within vascular channels was also associated with greater chondropathy ($Z = 2.4$, $P = 0.04$).

Inflammatory cells

CD3-positive lymphocytes were localized within subchondral bone spaces in each disease group and occasionally within vascular channels. Only cases with RA displayed CD3-positive cells in those vascular channels that invaded the articular cartilage (Fig. 2A). CD3-positive cells in subchondral bone spaces displayed heterogeneity between disease groups ($\chi^2 = 15.4$, $P = 0.004$), being increased in both RA and OA, and most abundant in RA (Table 1).

CD68-positive mononuclear cells in subchondral bone spaces and vascular channels displayed the appearance

TABLE 1 Clinical and pathological characteristics compared between RA, OA and PM controls

Clinical or pathological characteristic	RA	OA	PM
Age, years	68 (60–74)	61 (55–68)	50 (42–69)
Gender, female, %	80	27	55
Serum CRP, mg/l	**18 (11–26)**‡	<5 (<5–6)	NA
Radiography			
JSN (0–6)	4.8 (5–6)	5 (4.8–5.325)	NA
OSTs (0–12)	10 (8–12)	9 (8–10.3)	NA
General morphology			
Chondropathy (0–13)	**8.5 (5.5–10.3)***	8 (4–10)	4 (3–5)
Subchondral bone thickness, mm	**0.12 (0.11–0.17)***	0.17 (0.16–0.21)	0.18 (0.14–0.25)
Subchondral fibrovascular tissue (Y/N), %	**90****	55	18
Vascularity			
Vascular density, per mm			
Non-calcified cartilage	**0.45 (0.18–0.83)***	**0.42 (0.15–0.82)***	0.09 (0.07–0.19)
Calcified cartilage	0.80 (0.57–0.97)	0.71 (0.68–0.86)	1.2 (0.88–1.8)
Subchondral bone	**2.1 (0.6–2.6)****	**2.5 (1.6–4.0)***	5.3 (2.7–8.1)
EC proliferation			
Vascular channels, %	**55***	36	0
Subchondral spaces, %	55	45	11
Inflammatory cells			
CD3 subchondral spaces (0–2)	**2 (0.8–2)**,†	**0.5 (0–1)***	0 (0–0.8)
CD68 subchondral spaces (0–2)	1.5 (0.8–2)	1 (1–2)	1.5 (1–2)
Growth factor expression			
VEGF			
Subchondral spaces (0–2)	1 (0–2)	0 (0–1)	1 (0–2)
Channels (0–2)	0.5 (0–1)	0.5 (0–1)	1 (0–1)
Chondrocytes, %	27	**82***	18
PDGF			
Subchondral spaces (0–2)	1 (0–1)	0 (0–1)	0 (0–0)
Channels (0–2)	**2 (1–2)**,†	1 (0–1)	0 (0–1)
NGF			
Subchondral spaces, %	38	63	33
Channels (proportion positive)	**0.50 (0.08–0.69)***	**0.54 (0.05–0.79)***	0.14 (0.00–0.43)
Chondrocytes, %	100	75	78

Histological parameters are presented in subchondral bone spaces, vascular channels and (for VEGF and NGF), superficial chondrocytes. Values given as per cent indicate percentage of cases displaying that characteristic. Statistically significant differences between disease groups are highlighted in bold: RA or OA *vs* PM *$P < 0.05$, **$P < 0.01$; RA *vs* OA †$P < 0.05$, ‡$P < 0.01$. Values are median (IQR) for measurements and scores, or percentage of cases displaying the named characteristic. NA: not available.

of infiltrating macrophages (Fig. 2B), and were detected with similar frequency and density in all three disease groups (Table 1). Some CD68-positive multinucleated, osteoclast-like cells were observed. CD68-positive cells in vascular channels were more abundant in cases that displayed proliferating ECs in vascular channels ($Z = 2.1$, $P = 0.04$), but no other significant associations were detected between subchondral inflammatory cell infiltration and angiogenesis indices (Table 2).

Growth factors

VEGF-, PDGF- or NGF-positive cells were localized to blood vessels and non-vascular cells within vascular channels and subchondral bone spaces (Figs 3 and 4). PDGF- or NGF-positive cells were often adjacent to the bone surface. Vascular channels containing CGRP-immunoreactive nerve fibres also contained NGF-positive cells (Fig. 4E and F). VEGF, PDGF and NGF were also localized to chondrocytes. VEGF-positive chondrocytes were predominantly localized to the superficial zone of articular cartilage of OA cases (Fig. 3C) and NGF-positive chondrocytes were localized to superficial but not deep articular cartilage in all disease groups (Fig. 4D).

VEGF-positive superficial chondrocytes and PDGF- or NGF-positive cells in vascular channels each displayed heterogeneity between disease groups ($\chi^2 = 8.20$, $P = 0.02$; $\chi^2 = 12.9$, $P = 0.002$; $\chi^2 = 9.2$, $P = 0.01$, respectively). VEGF-positive chondrocytes were most common in OA; PDGF-positive cells in vascular channels were most abundant in RA; and vascular channels more commonly contained NGF-positive cells in OA and RA, than in PM (Table 1). VEGF and NGF expressions within vascular channels and VEGF expression by superficial chondrocytes were each associated with higher vascular densities in the non-calcified cartilage (Table 2).

Fig. 1 Morphology and vascularity at the osteochondral junction in RA, PM controls and OA. (**A**) General morphology at the osteochondral junction. RA: fibrovascular granulation tissue filling bone marrow spaces and invading the articular cartilage from below. There is proteoglycan loss and thinning of the articular cartilage and subchondral bone plate. Inset: blood vessel and inflammatory cells within the subchondral bone space. PM: normal cartilage, thick subchondral bone containing vascular channels and bone marrow spaces filled with fatty tissue. OA: fibrovascular tissue within a channel touching the tidemark (inset) as well as fibrillation, fissuring and proteoglycan depletion in cartilage at the articular surface. (**B**) Smooth muscle α-actin-positive cells (black) in subchondral bone spaces and associated vascular channels. Insets: positive blood vessels within a vascular channel (RA) and subchondral space (OA). (**C**) Vascular channels stained for CD34-positive ECs (red), PCNA-positive nuclei (black) and non-proliferating nuclei [4′-6′-diamidino-2-phenylindole (DAPI): fluorescent blue]. Proliferating ECs (long arrows) are demonstrated in a vascular channel that crosses the tidemark (broken line) in RA, and within the subchondral bone plate in OA. Proliferating non-ECs are also present (RA: short arrows). PM: vascular channel within the subchondral bone plate containing no proliferative ECs. Tissue morphology is revealed in (A) by Safranin O stain (red: proteoglycan; green: bone), with haematoxylin counterstain or (B and C) using combined transmitted and fluorescent light (blue/white: cartilage, bone and DAPI-reactive nuclei; yellow: background). Scale bars = 100 microns.

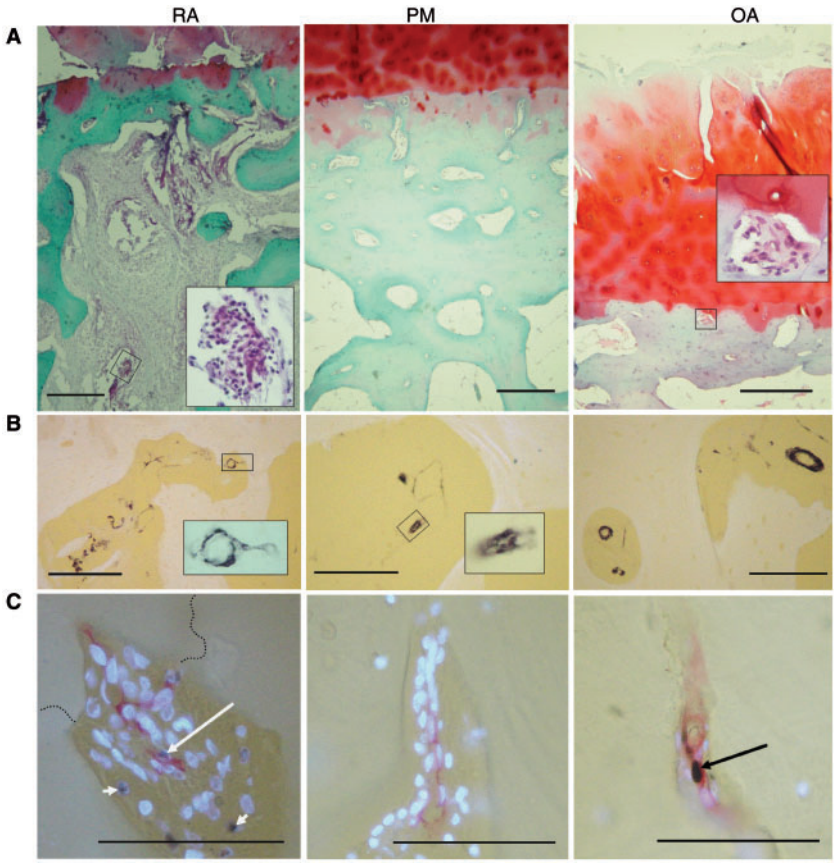

Discussion

Osteochondral angiogenesis was increased in RA and OA compared with non-arthritic knees, associated with both chondropathy and subchondral pathology. Our findings support the hypothesis that osteochondral angiogenesis is mediated by a pro-angiogenic environment within subchondral bone marrow spaces, enhanced in OA by angiogenic stimuli from articular chondrocytes. Osteochondral angiogenesis was also associated with increased NGF expression, and may facilitate the sensitization or growth into articular cartilage of sensory nerves. Our observational data from human tissues provide a basis for the validation of models of OA, which could be used to test the clinical implications and molecular mechanisms underlying associations between blood vessel and nerve growth.

Osteochondral angiogenesis

Vascularization of articular cartilage variously has been attributed to normal ageing [17, 31], loading [17] or OA and RA pathological change [8, 14, 16, 23, 32]. Standardized tissue collection from medial tibial plateaux

Table 2 Associations of vascular density in the non-calcified cartilage with morphology and cellular parameters at the osteochondral junction

	Non-calcified cartilage vascular density per millimetre			
	Parameter present	Parameter absent	*Z*-value	*R*-value
General morphology				
Cartilage score	–	–	–	**0.40***
Subchondral bone thickness	–	–	–	−0.38
Subchondral fibrovascular tissue	**0.34 (0.19–0.68)**	**0.15 (0.07–0.21)**	**−2.5****	–
Inflammatory cells				
CD68 subchondral spaces	–	–	–	−0.18
CD3 subchondral spaces	–	–	–	0.34
Growth factor expression				
VEGF				
Subchondral spaces	–	–	–	0.38
Channels	–	–	–	**0.45***
Chondrocytes	**0.57 (0.18–0.89)**	**0.16 (0.09–0.34)**	**−2.0***	–
PDGF				
Subchondral spaces	0.61 (0.17–0.83)	0.21 (0.14–0.62)	−1.1	–
Channels	–	–	–	0.28
NGF				
Subchondral spaces	0.25 (0.15–0.47)	−0.19 (0.02–0.55)	−0.7	–
Channels	–	–		**0.52****
Chondrocytes	0.20 (0.14–0.54)	0.08 (0.00–0.28)	−1.7	–

Vascular densities are given as median (IQR) for cases displaying (present) or not displaying (absent) dichotomous parameters, followed by *Z*-score for comparison by Mann–Whitney U-test. Associations between vascular density and continuous or ordinal parameters are given as Spearman's rank correlation coefficients. Histological parameters are presented in subchondral bone spaces, vascular channels and (for VEGF and NGF) superficial chondrocytes. Significant associations are highlighted in bold. $^{*}P < 0.05$, $^{**}P < 0.01$.

Fig. 2 Inflammatory cells in subchondral bone spaces and associated vascular channels. (**A**) CD3-positive lymphocytes (black) within fibrovascular tissue occupying subchondral bone spaces in RA and OA, but not in the fatty marrow of a PM control. Inset: subchondral bone space showing CD3-positive lymphocytes (arrows). Bo: bone; CC: calcified cartilage; NCC: non-calcified cartilage; broken line: tidemark. (**B**) CD68-positive cells (black) in RA, PM controls and OA. Mononuclear CD68-positive cells resembled macrophages and were localized either at the bone surface, or deeper within the subchondral bone space. Multinucleated CD68-positive cells localized at the bone surface (insets) resembled osteoclasts. Tissue morphology is revealed by combined transmitted and fluorescent light (blue/white: cartilage, bone; yellow: background). Scale bar = 100 microns.

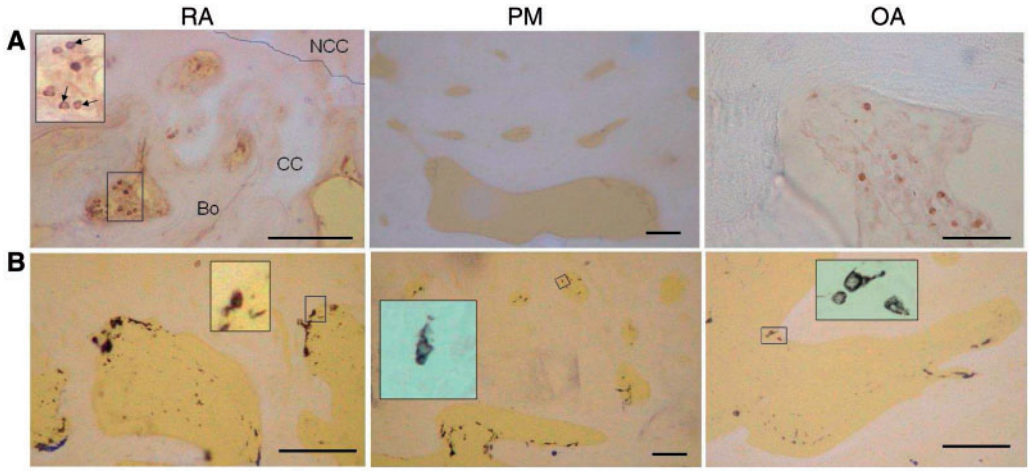

FIG. 3 Vascular growth factor expression in articular cartilage and bone. (**A**) VEGF-positive cells (brown) in vascular channels (RA, PM and OA), and in bone marrow spaces (RA). (**B**) PDGF-positive cells (brown). Vascular channels displaying PDGF-B-positive cells within the matrix and adherent to the bone surface in RA and OA, but not PM. (**C**) Chondrocytes displaying VEGF immunoreactivity in deep (RA) and superficial (OA) articular cartilage, but not in PM. Tissue morphology is revealed by combined transmitted and fluorescent light (blue/white: cartilage, bone; yellow: background) (**A** and **B**) or by haematoxylin counterstain (**C**). Scale bar = 100 microns.

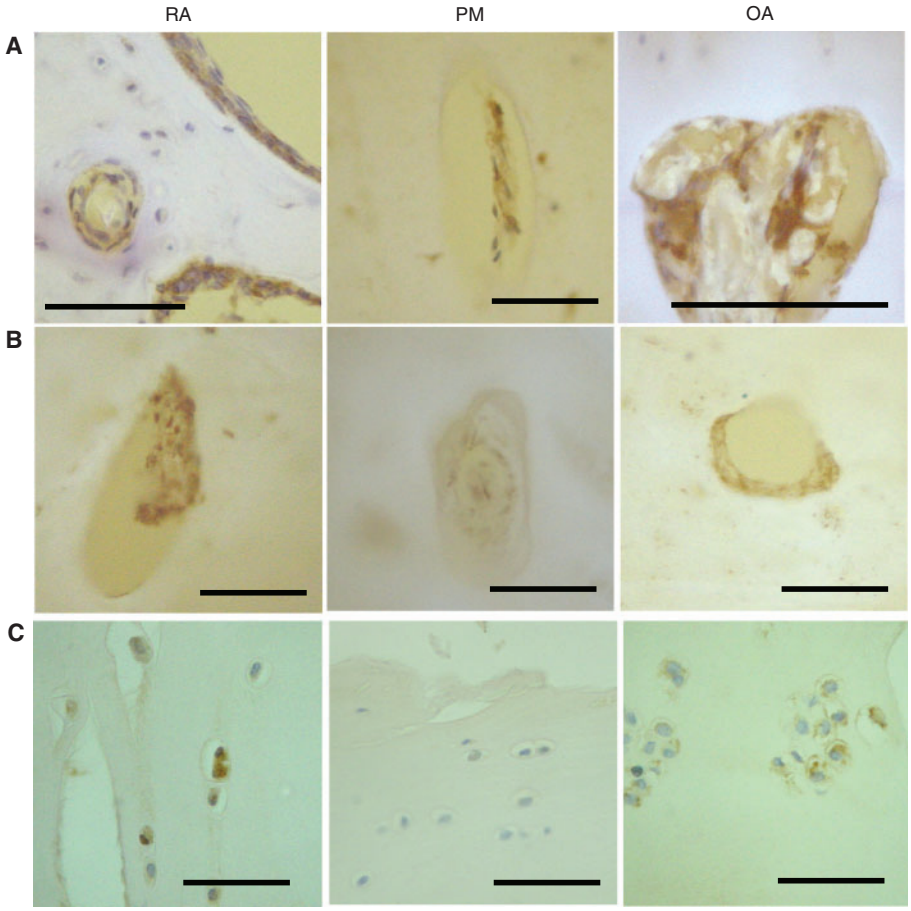

aimed to minimize differences in loading between cases in the current study. Associations between osteochondral vascularity and chondropathy are independent of ageing in animal models [33] and earlier data demonstrating increasing osteochondral vascularity from the seventh decade may be attributed to increasing prevalence of OA [31]. Our data support the hypothesis that increased vascularity in the non-calcified cartilage is a pathological feature of both OA and RA.

Vascular density in the non-calcified cartilage is a measure of osteochondral angiogenesis, as shown by its association with increased EC proliferation. Earlier methods inferring angiogenesis based on direct contact between channel contents and articular cartilage (open channels) [17, 31, 34] were not specifically associated with chondropathy [34], possibly due to confounding by sectioning artefacts and new bone deposition. We show that vascularity of the subchondral bone plate is decreased in diseased compared with control joints, probably due to a combination of thinning of the subchondral bone plate (in RA), and ossified channels that no longer contain soft tissue or evidence of vascularization [17]. In contrast, vascular channels breaching the tidemark were more abundant in diseased than in normal articular cartilage, and were associated with more severe chondropathy [16, 23].

Subchondral pathology and osteochondral angiogenesis

Fibrovascular replacement of adipose marrow tissue is a feature of both RA [1, 2, 11] and OA [1, 19]. Bone marrow lesions detected by MRI may sometimes reflect such marrow replacement, and have been associated with knee pain [35]. New blood vessels within the articular cartilage originate from subchondral bone marrow spaces, and we found that osteochondral angiogenesis was associated with fibrovascular marrow replacement. This may suggest that subchondral pathology drives vascular invasion into articular cartilage, or that angiogenesis or associated factors may stimulate fibrovascular marrow replacement. Fibrovascular marrow replacement also

FIG. 4 NGF expression in articular cartilage and bone. NGF-positive cells (brown) in vascular channels in the medial tibial plateau of patients with OA (**A**) and RA (**C**), but not in a non-arthritic control (**B**). (**D**) Chondrocytes displaying NGF immunoreactivity (brown) in superficial articular cartilage from a patient with OA (**E** and **F**). Co-localization within a vascular channel of NGF immunoreactivity (**E**, red) and a CGRP-immunoreactive nerve (**F**, black, arrow), demonstrated in serial tissue sections from a patient with OA. (**A–D**) DAB development with haematoxylin counterstain. (**E**) FastRed development. (**F**) Nickel-enhanced DAB development. Filled arrow heads: tidemark. Open arrow head: articular surface. Scale bar = 100 microns.

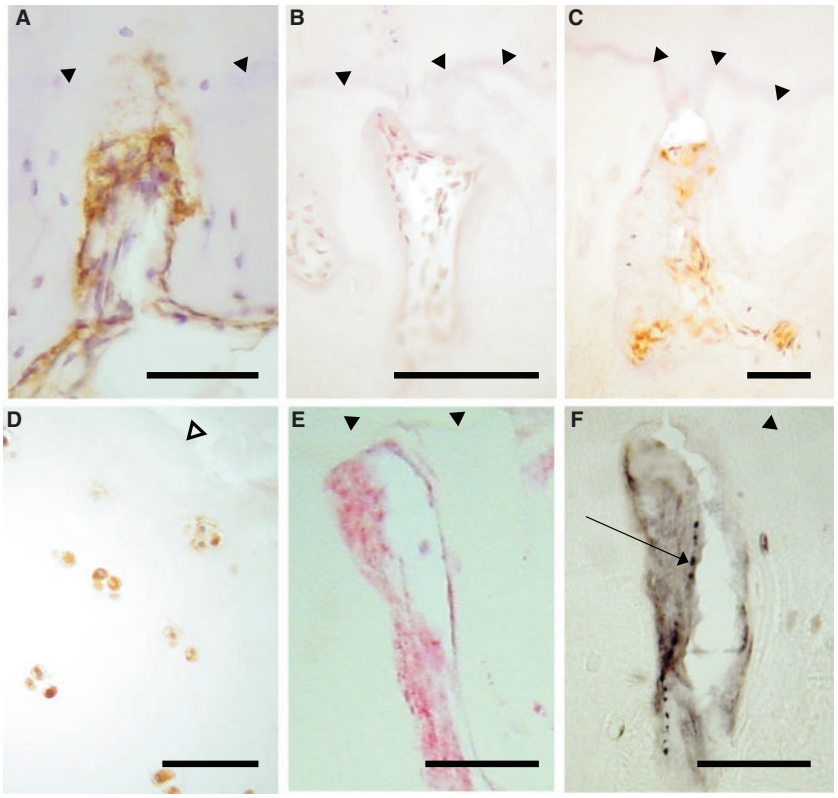

accompanies osteochondral vascular growth in the meniscal transection model of OA in rats [33], raising the possibility of testing the relationship between these phenomena in interventional studies.

Subchondral marrow replacement by fibrovascular tissue in RA previously has been compared with synovial pannus, containing lymphocytes and invading the articular cartilage through the subchondral bone plate [2, 11, 36]. Subchondral tissues are, however, distinct from synovium. Synovial pannus in OA typically does not invade cartilage [37], whereas subchondral vascular tissues invade into the non-calcified cartilage in both OA and RA. Synovial angiogenesis is associated with synovial macrophage infiltration [16, 22], whereas osteochondral angiogenesis was not associated with inflammatory cell infiltration in the current study. We previously did not find any association between osteochondral and synovial angiogeneses or synovitis in OA [16]. Subchondral tissues may influence osteochondral angiogenesis in ways that are distinct from the regulation of synovial vascular growth during synovitis.

Osteochondral angiogenesis in both RA and OA may be facilitated through the up-regulation of angiogenic factors within subchondral tissues. Angiogenic cytokines such as IL-1α, IL-8 and IL-10 have been localized to subchondral stromal cells both in RA and OA [21, 38], and we similarly demonstrate expression of both VEGF and PDGF. Increased expression of angiogenic factors by articular chondrocytes may also contribute to osteochondral angiogenesis [39]. The drive for osteochondral angiogenesis may differ between RA and OA, as suggested by our findings of higher expression of PDGF in RA and VEGF expression by superficial chondrocytes in OA.

NGF

Neovascularization of the non-calcified articular cartilage is associated with its innervation by fine, unmyelinated sensory nerves [8, 10]. We have demonstrated increased NGF immunoreactivity in patients with OA or RA compared with non-arthritic controls, colocalized with CGRP-immunoreactive nerve fibres within vascular channels. NGF expression was associated with osteochondral vascularity, and sensory nerve growth may be facilitated by the expression of NGF during osteochondral angiogenesis. Furthermore, NGF sensitizes nerves [40], such that increased NGF expression in RA and OA may

increase sensory nerve activity in the subchondral bone. Increased NGF production, therefore, may contribute to OA pain, both structurally (increased and aberrant innervation at the osteochondral junction), and through peripheral sensitization.

Nerve growth follows neovascularization in a variety of tissues, including subcutaneous sponge granulomas and healing fractures in animal models [41, 42]. Some growth factors, including NGF, may induce both blood vessel and nerve growth [26]. NGF produced by vascular cells may contribute to the growth of sensory nerves along newly formed vessels. However, the expression of NGF by non-vascular cells within vascular channels may suggest a more general stimulation of nerve growth, with direction along the neovasculature perhaps determined by other, as yet undefined, factors.

Interpretation of our findings is limited by a number of factors. Cross-sectional observational studies such as ours cannot prove causality. Immunohistological differences between PM and arthritic samples may have been confounded by PM tissue changes. However, such changes would be unlikely to influence comparisons between RA and OA, or structural components such as osteochondral vascular density, fibrovascular marrow replacement or bone plate thickness. Although not statistically significant, the PM group had a lower median age than either arthritic group. The high prevalence of OA in older populations makes age matching of PM samples difficult, and we elected in this study, by excluding all PM cases with macroscopic evidence of chondropathy, to avoid disease group contamination in preference to selecting age-matched cases. These limitations may be addressed through interventional studies in validated animal models that reflect those changes observed in man.

Conclusions

Osteochondral angiogenesis is a complex process that may be moderated by cells in the subchondral bone spaces, and by chondrocytes. Our data support potential roles for VEGF and NGF in human arthritis, and identify angiogenesis and nerve growth at the osteochondral junction as putative targets for therapeutic intervention. However, observational studies on human tissues can only support, rather than prove, hypothesized contributions of angiogenesis and nerve growth to clinical disease. Interventional studies are needed to determine whether neurovascular growth at the osteochondral junction may be a useful therapeutic target.

Rheumatology key messages

- Neurovascular growth is associated with VEGF, PDGF and NGF expression at the osteochondral junction.
- The osteochondral angiogenic milieu differs between RA and OA, and from that supporting synovial vascular growth.

Acknowledgements

We are grateful to all the patients, the orthopaedic surgeons and the Bereavement Centre at the Sherwood Forest Hospitals NHS Foundation Trust for providing clinical material. We also thank Roger Hill and the histopathology personnel at the King's Mill Hospital for their help with processing of tissue samples.

Funding: We are grateful to AstraZeneca for financial support to assist the creation of the tissue repository used in this study. D.W. was funded by AstraZeneca. D.F.M. was funded by the Arthritis Research Campaign grant 14851. Funding to pay the Open Access publication charges for this article was provided by Arthritis Research UK.

Disclosure statement: The authors have declared no conflicts of interest.

References

1 Appel H, Kuhne M, Spiekermann S *et al*. Immunohistochemical analysis of hip arthritis in ankylosing spondylitis: evaluation of the bone-cartilage interface and subchondral bone marrow. Arthritis Rheum 2006;54:1805–13.

2 Bugatti S, Caporali R, Manzo A, Vitolo B, Pitzalis C, Montecucco C. Involvement of subchondral bone marrow in rheumatoid arthritis: lymphoid neogenesis and in situ relationship to subchondral bone marrow osteoclast recruitment. Arthritis Rheum 2005;52:3448–59.

3 Kaneko M, Tomita T, Nakase T *et al*. Expression of proteinases and inflammatory cytokines in subchondral bone regions in the destructive joint of rheumatoid arthritis. Rheumatology 2001;40:247–55.

4 Lisignoli G, Piacentini A, Cristino S *et al*. CCL20 chemokine induces both osteoblast proliferation and osteoclast differentiation: increased levels of CCL20 are expressed in subchondral bone tissue of rheumatoid arthritis patients. J Cell Physiol 2007;210:798–806.

5 Burr DB, Schaffler MB. The involvement of subchondral mineralized tissues in osteoarthrosis: quantitative microscopic evidence. Microsc Res Tech 1997;37:343–57.

6 Burr DB. The importance of subchondral bone in osteoarthrosis. Curr Opin Rheumatol 1998;10:256–62.

7 Rau R, Wassenberg S, Herborn G, Perschel WT, Freitag G. Identification of radiologic healing phenomena in patients with rheumatoid arthritis. J Rheumatol 2001;28:2608–15.

8 Suri S, Gill SE, Massena de Camin S, Wilson D, McWilliams DF, Walsh DA. Neurovascular invasion at the osteochondral junction and in osteophytes in osteoarthritis. Ann Rheum Dis 2007;66:1423–8.

9 Hukkanen M, Konttinen YT, Rees RG, Gibson SJ, Santavirta S, Polak JM. Innervation of bone from healthy and arthritic rats by substance P and calcitonin gene related peptide containing sensory fibers. J Rheumatol 1992;19:1252–9.

10 Wojtys EM, Beaman DN, Glover RA, Janda D. Innervation of the human knee joint by substance-P fibers. Arthroscopy 1990;6:254–63.

11 Bromley M, Bertfield H, Evanson JM, Woolley DE. Bidirectional erosion of cartilage in the rheumatoid knee joint. Ann Rheum Dis 1985;44:676–81.

12 Bromley M, Woolley DE. Chondroclasts and osteoclasts at subchondral sites of erosion in the rheumatoid joint. Arthritis Rheum 1984;27:968–75.

13 Norrdin RW, Kawcak CE, Capwell BA, McIlwraith CW. Calcified cartilage morphometry and its relation to subchondral bone remodeling in equine arthrosis. Bone 1999;24:109–14.

14 Mankin HJ, Dorfman H, Lippiello L, Zarins A. Biochemical and metabolic abnormalities in articular cartilage from osteo-arthritic human hips. II. Correlation of morphology with biochemical and metabolic data. J Bone Joint Surg Am 1971;53:523–37.

15 Duncan H. Cellular mechanisms of bone damage and repair in the arthritic joint. J Rheumatol 1983;11(Suppl.): 29–37.

16 Walsh DA, Bonnet CS, Turner EL, Wilson D, Situ M, McWilliams DF. Angiogenesis in the synovium and at the osteochondral junction in osteoarthritis. Osteoarthr Cartil 2007;15:743–51.

17 Woods CG, Greenwald AS, Haynes DW. Subchondral vascularity in the human femoral head. Ann Rheum Dis 1970;29:138–42.

18 Haywood L, McWilliams DF, Pearson CI *et al*. Inflammation and angiogenesis in osteoarthritis. Arthritis Rheum 2003;48:2173–7.

19 Milgram JW. Morphologic alterations of the subchondral bone in advanced degenerative arthritis. Clin Orthop Relat Res 1983;173:293–312.

20 McQueen FM, Ostendorf B. What is MRI bone oedema in rheumatoid arthritis and why does it matter? Arthritis Res Ther 2006;8:222.

21 Hulejova H, Baresova V, Klezl Z, Polanska M, Adam M, Senolt L. Increased level of cytokines and matrix metalloproteinases in osteoarthritic subchondral bone. Cytokine 2007;38:151–6.

22 Walsh DA, Wade M, Mapp PI, Blake DR. Focally regulated endothelial proliferation and cell death in human synovium. Am J Pathol 1998;152:691–702.

23 Shibakawa A, Yudoh K, Masuko-Hongo K, Kato T, Nishioka K, Nakamura H. The role of subchondral bone resorption pits in osteoarthritis: MMP production by cells derived from bone marrow. Osteoarthr Cartil 2005;13: 679–87.

24 Bonnet CS, Walsh DA. Osteoarthritis, angiogenesis and inflammation. Rheumatology 2005;44:7–16.

25 Aloe L, Manni L, Sebastiani G *et al*. Nerve growth factor in the synovia of patients with rheumatoid arthritis: correlation with TNF-alpha and IL-1 beta and possible functional significance. Clin Exp Rheumatol 1999;17:632–3.

26 Nico B, Mangieri D, Benagiano V *et al*. Nerve growth factor as an angiogenic factor. Microvasc Res 2008;75:135–41.

27 Walsh DA, Wilson D. Post-mortem collection of human joint tissues for research. Rheumatology 2003;42:1556–8.

28 Nagaosa Y, Mateus M, Hassan B, Lanyon P, Doherty M. Development of a logically devised line drawing atlas for grading of knee osteoarthritis. Ann Rheum Dis 2000;59: 587–95.

29 Stefanini M, De Martino C, Zamboni L, Stefanini M, De Martino C, Zamboni L. Fixation of ejaculated spermatozoa for electron microscopy. Nature 1967;216:173–4.

30 Shu SY, Ju G, Fan LZ. The glucose oxidase-DAB-nickel method in peroxidase histochemistry of the nervous system. Neurosci Lett 1988;85:169–71.

31 Lane LB, Villacin A, Bullough PG. The vascularity and remodelling of subchondrial bone and calcified cartilage in adult human femoral and humeral heads. An age- and stress-related phenomenon. J Bone Joint Surg Br 1977; 59:272–8.

32 Greenwald AS, Haynes DW. A pathway for nutrients from the medullary cavity to the articular cartilage of the human femoral head. J Bone Joint Surg Br 1969;51: 747–53.

33 Mapp PI, Avery PS, McWilliams DF *et al*. Angiogenesis in two animal models of osteoarthritis. Osteoarthr Cartil 2008;16:61–9.

34 Clark JM. The structure of vascular channels in the subchondral plate. J Anat 1990;171:105–15.

35 Felson DT, Chaisson CE, Hill CL *et al*. The association of bone marrow lesions with pain in knee osteoarthritis. Ann Inter Med 2001;134:541–9.

36 Wyllie JC. Histopathology of the subchondral bone lesion in rheumatoid arthritis. J Rheumatol 1983;11(Suppl.):26–8.

37 Shibakawa A, Aoki H, Masuko-Hongo K *et al*. Presence of pannus-like tissue on osteoarthritic cartilage and its histological character. Osteoarthr Cartil 2003;11: 133–40.

38 Lisignoli G, Toneguzzi S, Pozzi C *et al*. Chemokine expression by subchondral bone marrow stromal cells isolated from osteoarthritis (OA) and rheumatoid arthritis (RA) patients. Clin Exp Immunol 1999;116:371–8.

39 Enomoto H, Inoki I, Komiya K *et al*. Vascular endothelial growth factor isoforms and their receptors are expressed in human osteoarthritic cartilage. Am J Pathol 2003;162: 171–81.

40 Ma QP, Woolf CJ, Ma QP, Woolf CJ. The progressive tactile hyperalgesia induced by peripheral inflammation is nerve growth factor dependent. Neuroreport 1997;8: 807–10.

41 Walsh DA, Hu DE, Mapp PI, Polak JM, Blake DR, Fan TP. Innervation and neurokinin receptors during angiogenesis in the rat sponge granuloma. Histochem J 1996;28: 759–69.

42 Aoki M, Tamai K, Saotome K. Substance P- and calcitonin gene-related peptide-immunofluorescent nerves in the repair of experimental bone defects. Int Orthop 1994;18:31.